



## ЭКСПЕРИМЕНТАЛЬНЫЕ ИССЛЕДОВАНИЯ EXPERIMENTAL RESEARCHES

DOI 10.22363/1815-5235-2021-17-3-278-287  
 UDC 62-233.27

RESEARCH ARTICLE / НАУЧНАЯ СТАТЬЯ

### Experimental verification of new features of bearing operation under combined loading conditions

Valeriy V. Kirilovskiy\*, Yuri V. Belousov

Bauman Moscow State Technical University (National Research University), 5 2nd Baumanskaya St, bldg 1, Moscow, 105005, Russian Federation  
 \*kvv@bmstu.ru

#### Article history

Received: February 22, 2021  
 Revised: April 2, 2021  
 Accepted: April 21, 2021

**Abstract.** Bearing units of lifting machines, products of construction, road, aviation, space and other branches of technology are very important structural elements, since the failure of even one bearing can cause the failure of the entire product. The results of experimental verification of the theoretical model of bearing operation under combined loading conditions are presented. The behavior under load of bearing units in the most general case can be represented by a sequence of five design schemes, expressed in the form of five statically indeterminate beams. The purpose of the experiments was to test this model under real loading conditions. The experiments were based on the analysis of the geometric shape of the curved elastic line, which the shaft of the bearing assembly acquires under load. The experimental results confirmed the validity of the model and showed that the previously generally accepted model of a two-support beam is not implemented. The conclusion is confirmed that in responsible lifting machines, as well as in responsible products of construction, road, aviation, space and other branches of technology, it is impractical to calculate bearings according to the traditional method, since an erroneous value of bearing durability can be obtained, overestimated from 28.37 to 26.663.9 times.

**Keywords:** shaft supports, design scheme, reactions in supports

#### For citation

Kirilovskiy V.V., Belousov Yu.V. Experimental verification of new features of bearing operation under combined loading conditions. *Structural Mechanics of Engineering Constructions and Buildings*. 2021;17(3):278–287. <http://dx.doi.org/10.22363/1815-5235-2021-17-3-278-287>

### Экспериментальная проверка новых особенностей работы подшипников в условиях комбинированного нагружения

В.В. Кириловский\*, Ю.В. Белоусов

Московский государственный технический университет имени Н.Э. Баумана (национальный исследовательский университет), Российская Федерация, 105005, Москва, ул. 2-я Бауманская, д. 5, стр. 1  
 \*kvv@bmstu.ru

#### История статьи

Поступила в редакцию: 22 февраля 2021 г.  
 Доработана: 2 апреля 2021 г.  
 Принята к публикации: 21 апреля 2021 г.

**Аннотация.** Подшипниковые узлы грузоподъемных машин, изделий строительной, дорожной, авиационной, космической и других отраслей техники являются очень ответственными элементами конструкций, поскольку выход из строя даже одного подшипника может стать причиной отказа всего изделия. Пред-

Valeriy V. Kirilovskiy, Associate Professor, Department of Bases of Machine Design, PhD (Technical Sciences); eLIBRARY SPIN-code: 4512-5571.  
 Yuri V. Belousov, Associate Professor, Department of Bases of Machine Design, PhD (Technical Sciences); Scopus Author ID: 57192978540, eLIBRARY SPIN-code: 7102-6966.  
 Кириловский Валерий Владимирович, доцент, кафедра основ конструирования машин, кандидат технических наук; eLIBRARY SPIN-код: 4512-5571.  
 Белоусов Юрий Вениаминович, доцент, кафедра основ конструирования машин, кандидат технических наук; Scopus Author ID: 57192978540, eLIBRARY SPIN-код: 7102-6966.

© Kirilovskiy V.V., Belousov Yu.V., 2021

This work is licensed under a Creative Commons Attribution 4.0 International License  
<https://creativecommons.org/licenses/by/4.0/>

**Для цитирования**

Кириловский В.В., Белоусов Ю.В. Экспериментальная проверка новых особенностей работы подшипников в условиях комбинированного нагружения // Строительная механика инженерных конструкций и сооружений. 2021. Т. 17. № 3. С. 278–287. <http://dx.doi.org/10.22363/1815-5235-2021-17-3-278-287>

ставлены результаты экспериментальной проверки теоретической модели работы подшипников в условиях комбинированного нагружения. Поведение под нагрузкой подшипниковых узлов в наиболее общем случае может быть представлено последовательностью из пяти расчетных схем, выраженных в виде пяти статически неопределимых балок. Целью проведения экспериментов явилась проверка данной модели в условиях реального нагружения. Эксперименты были построены на анализе геометрической формы изогнутой упругой линии, которую приобретает вал подшипникового узла под нагрузкой. Полученные результаты подтвердили справедливость модели и показали, что использовавшаяся ранее общепризнанная модель двухопорной балки не реализуется. Подтвержден вывод о том, что в ответственных грузоподъемных машинах, а также в ответственных изделиях строительной, дорожной, авиационной, космической и других отраслей техники нецелесообразно рассчитывать подшипники по традиционной методике, поскольку может быть получено ошибочное значение долговечности подшипников, завышенное от 28,37 до 26663,9 раз.

**Ключевые слова:** опоры валов, расчетная схема, реакции в опорах

## Introduction

Increased requirements for long-term trouble-free operation are imposed on the bearing units of lifting machines, as well as to the units of critical products in the construction, road, aviation, space and other branches of technology, since they must operate in the widest range of external operating conditions – from normal to critical and maximum permissible. In all cases, the calculation of the strength of the bearing units is reduced to the calculation of the durability of the standard bearings used in this units. It is very important to have accurate and reliable information about the forces acting on the bearings, because in any, even the most unfavorable external conditions, it is these forces that cause the bearings to malfunction and, accordingly, they determine their durability.

The forces acting on the bearings are the reactions in the supports of the beam, which is used as a design model in relation to a given bearing unit. The traditional, generally accepted design model for calculating and designing bearing units is a two-support beam, i.e. a smooth beam mounted on two hinged supports (Figure 1, *a*). When this beam deflects under the action of an external radial force  $F_r$  directed downward, its free ends rise upward, and the cross-sections located on the supports make a hinge rotation at a certain angle  $\alpha$ . In this case, one radial reaction occurs at a time on each support  $R_A$  and  $R_D$ .

However, at the N.E. Bauman Moscow State Technical University developed a theoretical model of the internal interaction under load of the parts of single-row radial ball bearings installed according to the spur pattern [1]. The model covers the most general conditions of combined loading, including axial  $F_a$  and continuously increasing radial  $F_r$  forces. In accordance with this model, the behavior of bearing units is most adequately described by a sequence of five design models, expressed in the form of five statically indeterminate beams. We call three of these five models the main ones – seal with an additional hinged support (Figure 1, *b*), double-sided seal (Figure 1, *c*), two double hinged supports (Figure 1, *d*). And the other two we call intermediate or transitional models – double hinged support on the left, simple hinged support on the right (Figure 1, *e*) and double hinged support on the left, seal on the right (Figure 1, *f*). The specified theoretical model justifies the development of several design models by the fact that, under conditions of combined load, the nature of the interaction of bearing parts does not remain constant and changes, therefore, the functions of the supports that the bearings perform under load are also modified and converted from one type of support to another type. It was found that the specific type of design model (type of beam) that can be applied to a given bearing unit depends on the magnitude of the radial force  $F_r$ . In turn, the composition, magnitude and direction of reactions in supports depend on the type of design model. And the nature of the reactions depends on the durability of the bearings, therefore the type of the design model is a very important, if not the primary in importance, characteristic in the calculation and design of bearing units.

Due to the fact that bearing units for general engineering applications operate under statically indeterminate design models, the loads acting on the bearings (reactions in the bearings) will actually be greater than the traditional design model of a two-support beam suggests. Therefore, the traditional bearing design method based on this two-support beam overestimates the durability values. The variance between the calculated and actual resource can reach 50 to 100 times [2]. This is a major disadvantage of the traditional bearing design method. Earlier, to explain this discrepancy, a large number of assumptions were made, based on important, but not primary factors. In accordance with one of them, the discrepancy is associated with the features of the condition of the oil layer, its contamination and other parameters, therefore it was proposed to introduce additional coefficients into

the calculation dependencies given in the international standard ISO 281: 2007 “Dynamic load ratings and rating life” features. The necessity to take these parameters into account under constant and variable loading conditions is reflected in GOST 18855–2013, as well as in the works of famous scientists [3–4]. Additionally, contact interactions in bearings were studied [5–7] in order to increase their service life and carrying capacity [8–11].

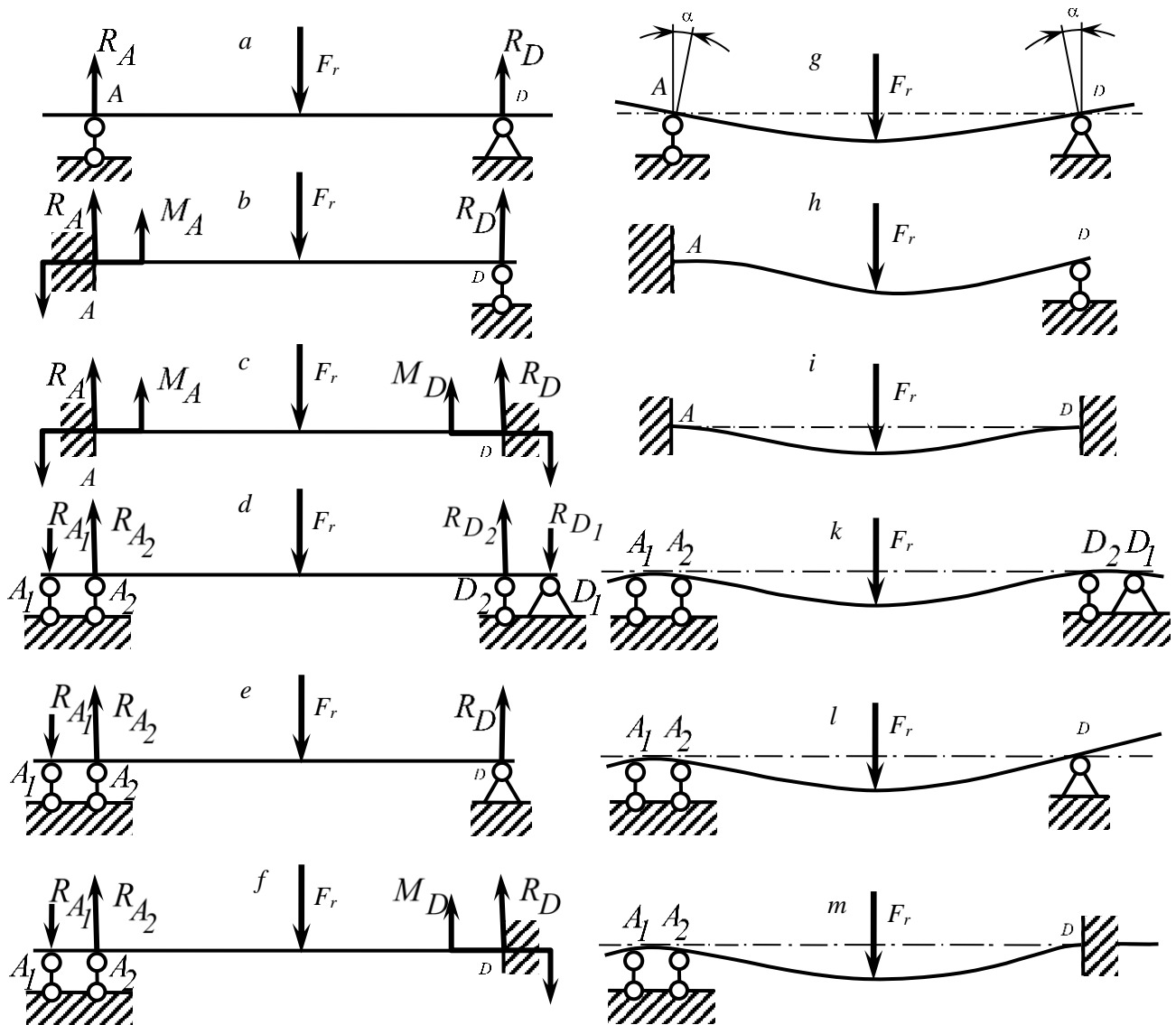


**Figure 1.** Reactions in the supports and the shape of the elastic line of the beams before (a–f) and after deformation (g–m):  
a – statically definable two-support beam; b–f – statically indeterminate beams

The regularities of the formation and accumulation of fatigue microdamages in the surface layer of the raceways were investigated in the publications [12; 13]. In addition, publication [13] proposes an interesting but very laborious method for repairing the properties of a layer with accumulated microdefects. This method can be applied to machines of unique design with very expensive bearings. Its content lies in the fact that by removing the defective layer, further unfavorable development of microdefects can be prevented. For this, it was proposed to disassemble the bearing, additionally regrind the raceways to a depth that ensures the removal of the defective layer, and then assemble it with new rolling elements, the diameter of which is increased in comparison with the original diameter by the thickness of the metal layer that removed by regrinding.

A wide range of studies are known based on the finite element method (FEM) [14–18]. The topics of these publications are similar or close to publications [5–11]. Studies [14–18] allowed to summarize a large amount of information about the operation of bearings in various operating conditions and confirmed the results obtained earlier.

A separate group of publications are studies devoted to monitoring the operation of bearings directly as part of an operating unit [19–24]. Monitoring is carried out in the form of continuous or discrete (periodic) diagnostics of bearings, which makes it possible to monitor the development of microdamages in raceways, to predict in a timely manner the impending failure of the bearing and thereby prevent its possible adverse consequences. There are many methods for bearing diagnostics. One of the most promising is the method based on the analysis of acoustic emission signals arising from the movement of rolling elements along the raceways.

In [20], a method based on the analysis of the sparse decomposition of K-means is considered, which includes an algorithm for searching for a sparse adaptive correspondence and an iterative method based on the minimum similarity of the atomic structure. This makes it possible to reliably extract and process the useful signal from a flow of complex arbitrary vibration signals. The method is useful for detecting minor bearing damage in the early stages of its occurrence.

In [21], it was proposed to register the early nucleation of microdefects by the method of pulsed amplification of the characteristics of the sparse representation, which makes it possible to improve the signal-to-noise ratio for a weak acoustic emission signal.

In [22], a method for extracting a useful signal using the structure of symbolic aggregate approximation (SAX) is proposed for similar purposes. This method takes into account the bearing loading conditions based on a two-support beam.

For effective recognition of acoustic emission signals indicating the development of microdefects, it is additionally proposed to use the Thomson multiparameter periodogram [23] or the empirical wavelet transform [24].

The studies listed above provide very important, useful and interesting material for the analysis of the operation of bearings. They point to a large number of different aspects that affect the design or actual life of the bearings. However, most likely, the reason for the variance between the calculated and actual life lies precisely in the more severe than previously assumed operating conditions of the bearings and the higher loads acting on them.

### The aim of the experiments

Two aims were set during the experiments:

- to check, under real loading conditions, whether radial single-row ball bearings installed according to the spur pattern fulfill the function of traditional pivot bearings or whether a model based on statically indeterminate design models is valid;
- to decide the question of whether the type of supports, the functions of which are performed by the bearings during loading, is constant, or whether they are modified and converted from one type to another.

### Method of experimental study

The method of experimental study was based on the analysis of the geometric shape of a curved elastic line, which is acquired by the shaft of the bearing assembly under load (Figure 1,  $g-l$ ). The idea behind the experiments is based on a simple and very reliable fact. The type of support, the function of which the bearing performs at the moment of loading, can be unambiguously established by the direction of movement in the space of the free end of the shaft, near which this bearing is installed.

So, if, under the action of a radial force directed downward, the end of the shaft (beam) rises up, the bearing closest to this end acts as a hinge support. In Figure 1,  $h$  or  $l$  is the right end, and in Figure 1,  $g$  – both ends of the shaft. If the free end of the shaft (beam) is stationary in space, the bearing in the design diagram can be represented by a seal (left end in Figure 1,  $h$ , right end in Figure 1,  $m$ , or both ends in Figure 1,  $i$ ). If the end of the shaft goes down, the nearest bearing can be represented by a double pivot bearing (Figure 1,  $k-m$ ).

The study was carried out in the following order (Figure 2). Shaft (1) with two exit ends was mounted on single-row deep groove ball bearings (2 and 3) according to the spur pattern. A continuously increasing radial load  $F_r$  was applied in the middle part of the shaft by moving the screw press rod, on which the pusher (4) was installed. The axial load  $F_a$  was applied using an adjustable threaded stopper (5), which, when unscrewed, acted on the stationary press column (6) through the ball (7). The movements of the left and right ends of the shaft were measured using the left (8) and right (9) indicators.

The object of study was a cylindrical single-stage gearbox (1) (Figure 3), in which its experimental models with two exit ends were used as a drive shaft (Figure 4,  $b$ ). Shaft samples were mounted on bearings 305 according to the spur pattern. The gearbox was fixed on the Table 2 (Figure 3) of the screw press (3) and, with the help of the threaded stopper (4), the central axial force  $F_a$  was applied to the left end of the investigated shaft. Then, by moving the pusher (5), a radial load  $F_r$  was applied in the middle part of the shaft. The value of the radial force was determined

by the readings of the indicator (6) of the dynamometer (7). The vertical displacements (bending) of the left and right exit ends of the shaft were controlled by the left (8) and right (9) indicators. Samples of the drive shaft with four different values of the bending stiffness in the middle part were used in the study (Figure 4, *b*). Studies using a similar method, but in a reduced volume, were carried out by us earlier with one fixed value of the shaft stiffness [25].

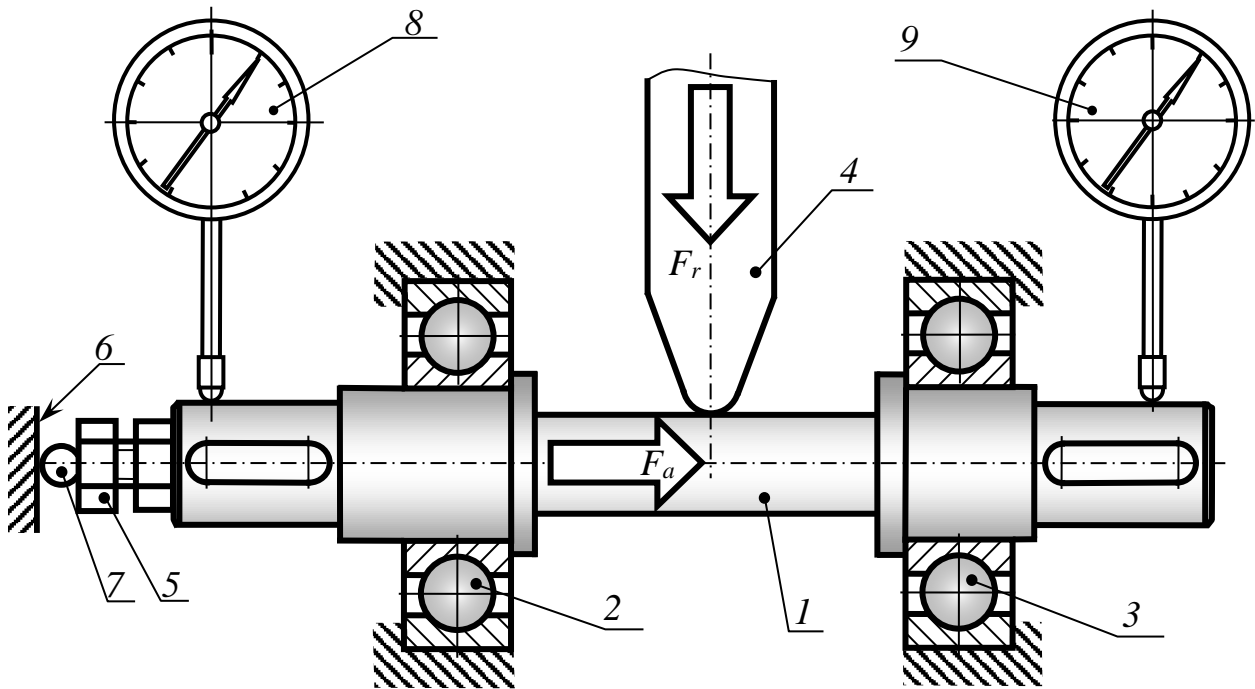


Figure 2. Model of experimental study

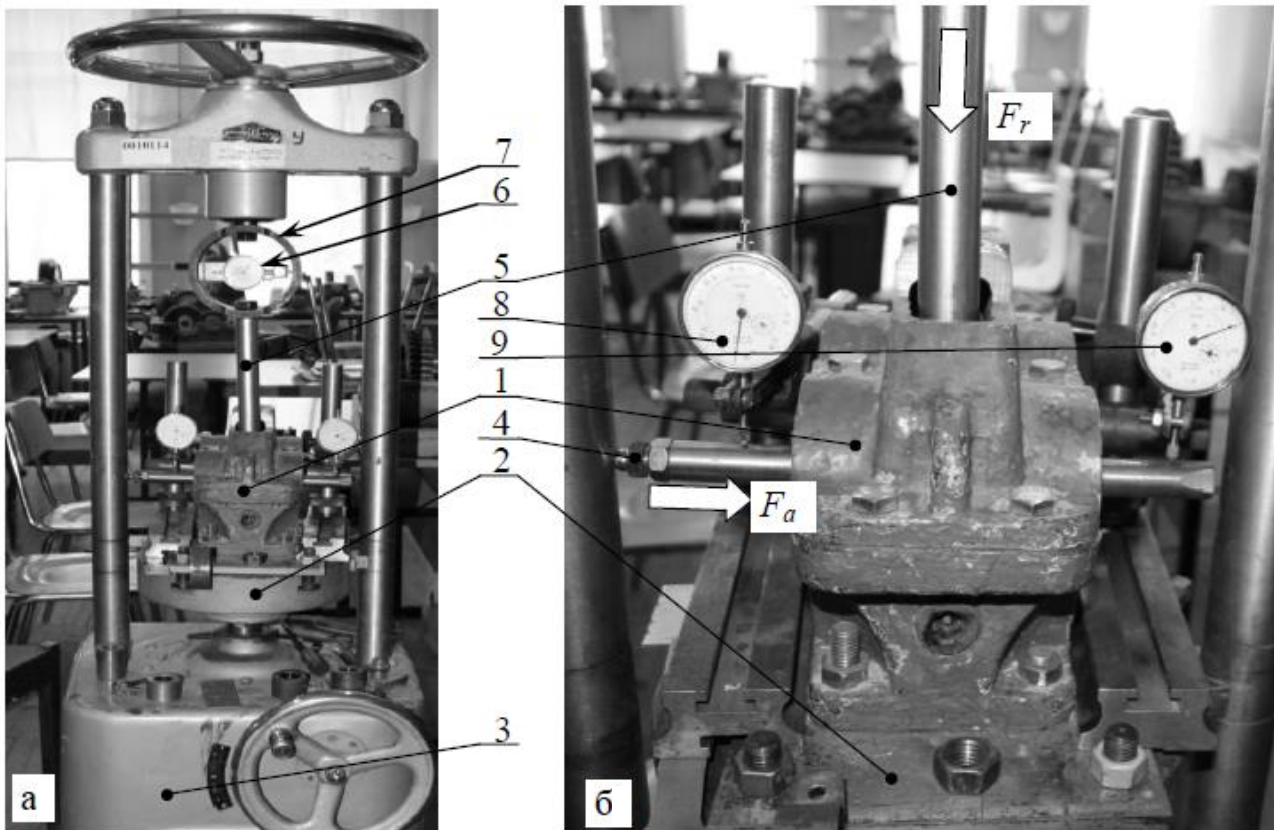


Figure 3. Experimental setup (photo by V.V. Kirillovskiy):  
*a* – general view of the press; *b* – the gearbox under study

### Results and discussion

The graphs of Figure 4, *a* reflect the dependency of the bending  $\Delta$  of the left and right ends of the experimental shafts on the value of the radial force  $F_r$ . The lines on the graph are numbered 1, 2, 3 and 4. Each line corresponds to a certain stiffness of the shaft. The graph numbered 1 corresponds to a shaft whose diameter in the middle section is 15 mm (Figure 4, *b*). In the group of shafts under study, the stiffness of this shaft was minimal. Line 2 corresponds to a diameter of 20 mm, line 3 to a diameter of 25 mm, and line 4 to a diameter of 30 mm.

For a more visual perception of the shape of the graphs, we have drawn four abscissa axes with their upward displacement relative to each other by one division of the  $\Delta$  scale. Similarly, the graphs themselves were shifted (i.e., they formed four origin of coordinates). Otherwise, all four graphs starting at one point would partially merge and make it impossible to clearly perceive their shape.

We used the part of the field located to the left of the ordinate axis to represent the bending of the left ends of the shafts, and the right part – for the right ones. The values of the radial force  $F_r$  were plotted on the abscissa axis to the left and to the right. These values on both branches of the axis are designated by points 1, 2, ..., 13. The numbers correspond to the number of indicator divisions 6 (Figure 3). Thus, points with the same numbers on the left and on the right correspond to the same values of the radial force  $F_r = Nk$ , where  $N$  is the point number,  $k$  is the proportionality coefficient of the dynamometer 7 ( $k = 311 \text{ N}$  in accordance with the manual of the press).

The bending values, directed upwards, were plotted on the positive branch of the ordinate axis, and those directed downward, on the negative one. The division value of  $\Delta$  scale is 0.02 mm (corresponds to the division value of the indicator 6, Figure 3).

The experimental results fully confirmed the provisions of the theoretical model. The predicted statically indeterminate design models were most pronounced at the minimum stiffness of the shaft (this is line number 1 – the diameter of the shaft in the middle section is 15 mm). Using this graph as an example, we will consider its features in more detail.

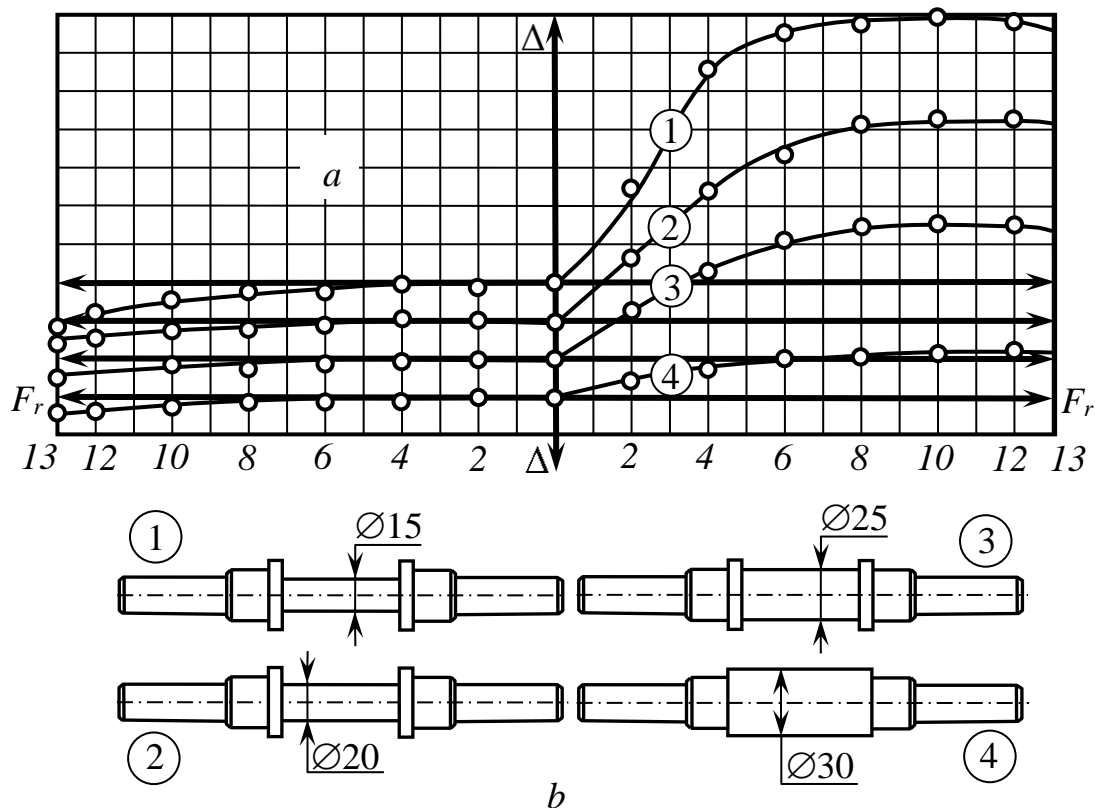


**Figure 4.** The results of experimental studies:  
*a* – the nature of the vertical movements of the shaft ends at different values of the radial force  $F_r$ ;  
*b* – sketches of the studied shafts of different stiffness

As the radial force  $F_r$  increased from point 0 to point 4 ( $0 < F_r < 1244 \text{ N}$ ), the left end of the shaft remained motionless. Therefore, this bearing in the specified range of values of the radial force performed the function of

a seal. Fixation of the shaft end in space was ensured by reactions that occurred in the bearing. Further, starting from point 4 and up to point 13 ( $1244\text{ N} < F_r < 4043\text{ N}$ ), the left end went down. I.e., in this range of  $F_r$ , the reactions in the left bearing increased to such an extent that they overcame the resistance of the left end of the shaft and elastically bent it down. This means that in the specified range  $1244\text{ N} < F_r < 4043\text{ N}$ , the seal function, which the left bearing previously performed, has been converted into the function of a double pivot bearing.

At the same time, the right end from point 0 to point 8 ( $0 < F_r < 2488\text{ N}$ ) went up (the right bearing served as a pivot bearing), from point 8 to point 11 ( $2488\text{ N} < F_r < 3421\text{ N}$ ) remained practically motionless (the pivot bearing was transformed into a seal), and from point 11 to point 13 ( $3421\text{ N} < F_r < 4043\text{ N}$ ) went down (the seal was transformed into a double hinge support). Thus, from point 1 to point 4, the original design model developed “to the left of the seal, to the right of the hinge support”, from point 4 to point 8 – the intermediate transitional model “on the left is a double hinge support, on the right is a conventional hinge support”, from point 8 to point 11 – another intermediate transitional model “left double pivotal support, on the right seal”, from point 11 to point 13 – the final main model “two double pivotal support”. Consequently, the position of the theoretical model on the possible implementation of intermediate transient design models was also confirmed. The formation of such intermediate calculation models is explained as follows. The transformation of any current type of support into a subsequent one cannot occur instantly. This transformation requires a certain finite period of time. In addition, transformations in the left and right supports cannot occur at the same time. Therefore, it seems quite natural that such a transformation has already been completed in one bearing (for example, in the left bearing), while in the other it has not yet begun (for example, in the right bearing).

It can be seen from the graphs that the stiffness of the shaft has a significant effect on the type of the design model. With an increase in stiffness (lines 2, 3, 4), the transition from the original model (“seal with an additional hinge support”) to the later current design models shifts to the area of increased values of the radial force, i.e., the transition occurs with a delay in comparison with low stiffness. With a diameter in the middle section of the shaft of 20 mm (line 2), the transition to the left of the seal to the double hinged support occurred approximately at point 5 ( $F_r = 1555\text{ N}$ ), at  $\varnothing 25\text{ mm}$  (line 3) – at point 6 ( $F_r = 1866\text{ N}$ ), for  $\varnothing 30\text{ mm}$  (line 4) – at point 7 ( $F_r = 2177\text{ N}$ ). And on the right, the transition from the hinged support to the seal occurred: at  $\varnothing 20\text{ mm}$  – at point 9 ( $F_r = 2799\text{ N}$ ); at  $\varnothing 25\text{ mm}$  – at point 10 ( $F_r = 3110\text{ N}$ ); at  $\varnothing 30\text{ mm}$  – at point 11 ( $F_r = 3421\text{ N}$ ).

### ***Discussion of the results***

1. During the experiments, indicators 8 and 9 (Figure 2), installed at the ends of the shafts, measured the total displacements  $\Delta_\Sigma$ , which consisted of several elementary displacements:  $\Delta_\Sigma = \Delta_1 + \Delta_2 + \Delta_3$ , where  $\Delta_1$  is the elastic deflection of the shaft end under the action of an external load, the size and direction of  $\Delta_1$  depend on the type of support, which at the moment of loading is performed by the bearing closest to this exit end of the shaft, as well as on the bending stiffness of the shaft;  $\Delta_2$  is the subsidence of the shaft, as a rigid body, as a result of contact deformation of bearing parts;  $\Delta_3$  is the subsidence of the gearbox body as a result of elastic deformation of the bearing seats (holes in the body) under load. It is of great interest what is the proportion of  $\Delta_1$ , deflections of the shaft ends, in the obtained values of  $\Delta_\Sigma$ .

2. The following can be said about  $\Delta_2$  and  $\Delta_3$ . The value of  $\Delta_2$  cannot exceed the limits for the dimensions of the raceways, as well as the limits for the shape and location of these surfaces. In turn, the value of  $\Delta_3$  cannot exceed the values of limits for dimensions and values of limits for the shape and location of the surfaces of the bearing seats in the body. The specified limits are established by GOST 520–2011 and GOST 3325–85. If, as a result of contact deformation of the bearing seats or bearing rings, the parameters specified in GOST are exceeded, the bearing assembly will be deemed unsuitable for operation. Standard limits of bearings 305 used in the experiment, as well as limits of bearing seats, are in the range of 0.005 to 0.01 mm.

By installing additional indicators at various points of the gearbox body, and, first of all, in the area of the lugs, we made sure that the value of  $\Delta_3$  did not exceed in the experiments the values of hundredths of a mm.

Further, if we estimate, for example, the values of  $\Delta_\Sigma(8)$  for the right end of the shaft at point 8 (Figure 4, a), in which  $\Delta_\Sigma(8) \approx 0.14\text{ mm}$ , we can say that  $\Delta_\Sigma(8)$  is 14 to 28 times more than possible values of  $\Delta_2$  and  $\Delta_3$ . This shows that  $\Delta_1$  (bending) is the main contributor to the value of  $\Delta_\Sigma(8)$ .

In addition, when the shaft end bends, its position becomes inclined. We installed two indicators at the left and right output ends – at the beginning and at the end of the corresponding exit section to check whether the end of the shaft sags in parallel, like a rigid body, as a result of contact deformations, or if its position as a result of bending becomes inclined and its angle of inclination increases with an increase in the external radial force. The readings of the indicator at the end of the exit section always (except for the seal condition) were lar-

ger and increased to a greater extent than at its beginning, which indicated precisely the angular displacements of the ends. When the shaft subsided as a rigid body, the readings of the indicators at the beginning and at the end of the sections would change identically.

Thus, it can be argued that the readings of the indicators presented in the graphs in Figure 4, *a*, contain mainly the values of  $\Delta_1$ , i.e., the values of the bending of the ends of the shafts.

### Conclusion

The carried out experimental studies have confirmed the main provisions of the theoretical model, which are as follows:

a) the traditional design model of a two-support beam is not implemented, when loaded with a combined load of ball radial single-row bearings installed in a spindle;

b) under conditions of combined loading with a continuously increasing radial force  $F_r$ , a sequential transformation of the three main statically indeterminate design models is realized, starting from the “seal with an additional hinged support” model, through a possible “double-sided seal” model to the final model “two double hinged supports”;

c) the functions of the supports, which the bearings perform during the loading process, are not constant and can be modified. So, in the left bearing, the original seal is converted into a double pivot bearing, and in the right bearing – the original pivot bearing is converted into a seal first, and only then into a double pivot bearing;

d) the time intervals during which the transformation of the current types of supports into subsequent ones occurs on the left and right, differ significantly from each other. Therefore, a situation is possible when, for example, on the left, the transformation of the embedment into a double pivot bearing has already been completed, and on the right, the pivot bearing or the embedding still continues to exist. Then, as experiments have confirmed, in addition to the main models, intermediate transitional design models can also develop – “double hinged support on the left, hinged support on the right” and “double hinged support on the left, seal on the right”. Thus, the behavior under load of the considered bearing units in the most general form can be described by a model that includes five design models – three main and two intermediate transition models.

Seals are short-term forms of supports and, in the future, if the bending stiffness of the shaft permits, they are converted into double hinged supports. This transformation takes place first at the left support. So,

with the bending stiffness of the shaft in the middle section  $EI = \frac{E\pi d^4}{64} = 521,9 \text{ MN}\times\text{mm}^2$  и and stiffness of

end section  $EI = 4026,7 \text{ MN}\times\text{mm}^2$  transition of the seal from the left to the double hinged support occurred in the experiments at the value of the radial force  $F_r = 1244 \text{ N}$ , and on the right – at  $F_r = 2488 \text{ N}$ .

The most complete sequence of design models is realized with a low bending stiffness of the shaft. This is the case for relatively thin and long shafts as well as thin-walled hollow shafts. With an increased stiffness of the shaft, the transition from the current design model to the next one occurs with an increased external radial load  $F_r$ . In the case of high bending stiffness, a variant is possible when the initial design model will also be final. Short shafts with relatively large cross-sectional diameters have high bending stiffness.

### Tasks for further study

1. The traditional method of calculating bearings for durability is based on the use of a design model of a two-support beam. This is expressed, first of all, in the fact that this method involves the action of one radial reaction on each bearing. In reality, for example, in the seal and double pivot bearing, several forces act on the bearing. In the future, it will be necessary either to develop a new method for calculating bearings, or to modify the existing one in order to adapt it to real statically indeterminate design models.

2. It is also likely that changes will be required in many of the traditionally established ideas about the operation, design, manufacture, testing and operation of bearing units, since these ideas are also based to one degree or another on a two-support beam.

3. It may be necessary to clarify the currently accepted, including internationally, concepts of static and dynamic radial load ratings of bearings, as well as change the values of these parameters given in the catalogs of bearing manufacturers.

This is explained as follows. The definition of the concept of static radial load capacity is established by the standards ISO 76:2006 and GOST 18854–2013, and the concept of dynamic radial load capacity is established by ISO 281:2007 and GOST 18855–2013. In accordance with these standards, the specified parameters

mean one static or one dynamic radial force of the maximum value, which, when acting on a bearing under standard loading conditions, can lead to the degree of damage specified by the standards.

Considering that not one, but several radial forces act on the bearing in the seal and the double pivot bearing, it is impossible, based on the current standards, to determine what force or what combination of forces is to be considered static or dynamic radial load capacity. In such a situation, the analytical expressions given in the standards for determining the durability of bearings lose their relevance. And also the calculated values of the static or dynamic radial load capacities, which are currently indicated by the bearing manufacturers in their catalogs, become unacceptable. Accordingly, analytical expressions and catalogs need to be revised and refined.

To do this, it will be necessary to establish the patterns of damage accumulation and collapse of the surface layer of the raceways and rolling elements as a result of their cyclic contact interaction in the process of mutual rolling, moreover, it is in the conditions of statically indeterminate models.

4. The loads acting directly on the bearing (reactions in the bearings) significantly depend on the conditions in which statically indeterminate design model the bearing operates, since the composition and values of the reactions in each of the models differ significantly from each other. Apparently, it will be advisable to indicate in the revised catalogs of bearings not one value of the static and one value of the dynamic radial load capacity, but five revised values – one for each specific design model.

5. It will be necessary to adjust the bearing test procedure in such a way as to carry out them separately for each statically indeterminate model and so that during any tests the conditions of their carrying out are guaranteed not to go beyond the required model.

### References

1. Kirilovskiy V.V., Belousov Yu.V. Theoretical substantiation of new features of rolling bearings operation under combined loading conditions. *RUDN Journal of Engineering Researches*. 2021;22(2):184–195. (In Russ.) <https://doi.org/10.22363/2312-8143-2021-22-2-184-195>
2. Nosov V.V. (ed.) *Bearing units of modern machines: an encyclopedic reference*. Moscow: Mashinostroenie Publ.; 1997. (In Russ.)
3. Ryakhovskiy O.A., Goncharov, S.Yu., Syromyatnikov V.S. Experimental determination of temperature in rolling bearings. *BMSTU Journal of Mechanical Engineering*. 2014;(10):3–9. (In Russ.)
4. Fomin M.V. Determination of equivalence coefficients for variable loading modes of gears and rolling bearings. *SPRAVOCHNIK. Inzhenernyi Zhurnal*. 2007;8(125):39–48. (In Russ.)
5. Matvienko Yu.G., Bubnov M.A. Contact interaction and destruction of the surface layer under conditions of rolling friction and jamming. *Problemy Mashinostroeniya i Nadezhnosti Mashin*. 2009;(4):43–49. (In Russ.)
6. Nakhatakyan F.G. Mechanics of contact convergence of elastic bodies in the Hertz problem. *Problemy Mashinostroeniya i Nadezhnosti Mashin*. 2010;(5):48–56. (In Russ.)
7. Nakhatakyan F.G. Calculation determination of elastic compliance of roller bearings on the basis of the Hertz theory]. *Problemy Mashinostroeniya i Nadezhnosti Mashin*. 2011;(1):28–32. (In Russ.)
8. Orlov A.V. Evaluation of the reliability of a ball bearing according to the criterion of clutch stability. *Problemy Mashinostroeniya i Nadezhnosti Mashin*. 2004;(4):77–83. (In Russ.)
9. Orlov A.V. The effect of wear on the performance of rolling bearings. *Problemy Mashinostroeniya i Nadezhnosti Mashin*. 2007;(5):71–79. (In Russ.)
10. Pavlov V.G. Service life of a deep groove ball bearing according to the condition of maximum permissible wear. *Problemy Mashinostroeniya i Nadezhnosti Mashin*. 2007;(6):102–111. (In Russ.)
11. Orlov A.V. Increasing the static load capacity of ball bearings. *Problemy Mashinostroeniya i Nadezhnosti Mashin*. 2009;(5):67–70. (In Russ.)
12. Vijay A., Sadeghi F. A continuum damage mechanics framework for modeling the effect of crystalline anisotropy on rolling contact fatigue. *Tribology International*. 2019;140:105845. <https://doi.org/10.1016/j.triboint.2019.105845>
13. Paulson N.R., Evans N.E., Bomidi J.A.R., Sadeghi F., Evans R.D., Mistry K.K. A finite element model for rolling contact fatigue of refurbished bearings. *Tribology International*. 2015;85:1–9. <https://doi.org/10.1016/j.triboint.2014.12.006>
14. Golmohammadi Z., Sadeghi F. A 3D finite element model for investigating effects of refurbishing on rolling contact fatigue. *Tribology Transactions*. 2020;63(2):251–264. <https://doi.org/10.1080/10402004.2019.1684606>
15. Weinzapfel N., Sadeghi F., Bakolas V. A 3D finite element model for investigating effects of material microstructure on rolling contact fatigue. *Tribology and Lubrication Technology*. 2011;67(1):17–19.
16. Belousov Y.V., Rekach F.V., Shambina S.L. Modelling of the tools' power interaction during mechanical machining by cutting. *International Journal of Recent Technology and Endineering*. 2018;7(4):132–134.

17. Abdullah M.U., Khan Z.A., Kruhoeffler W., Blass T. A 3D finite element model of rolling contact fatigue for evolved material response and residual stress estimation. *Tribology Letters*. 2020;68:122. <https://doi.org/10.1007/s11249-020-01359-w>
18. Bogdański S., Trajer M. A dimensionless multi-size finite element model of a rolling contact fatigue crack. *Wear*. 2005;258(7–8):1265–1272. <https://doi.org/10.1016/j.wear.2004.03.036>
19. Jiaxian C., Wentao M., Yuejian Ch. Transferable health indicator for rolling bearings: a new solution of cross-working condition monitoring of degradation process. *2020 Asia-Pacific International Symposium on Advanced Reliability and Maintenance Modeling (APARM)*. 2020:1–6. <https://doi.org/10.1109/APARM49247.2020.9209439>
20. Wang H., Du W. A new K-means singular value decomposition method based on self-adaptive matching pursuit and its application in fault diagnosis of rolling bearing weak fault. *International Journal of Distributed Sensor Networks*. 2020;16:155014772092078. <https://doi.org/10.1177/1550147720920781>
21. Lin H., Wu F., He G. Rolling bearing fault diagnosis using impulse feature enhancement and nonconvex regularization. *International Journal of Mechanical Systems and Signal Processing*. 2020;142:106790. <https://doi.org/10.1016/j.ymssp.2020.106790>
22. Smith W.A., Randall R.B. Diagnostics using the case western reserve university data: a benchmark study. *Mechanical Systems and Signal Processing*. 2015;64–65:130–131. <https://doi.org/10.1016/j.ymssp.2015.04.021>
23. Gaikwad J.A., Gholap Y.B., Kulkarni J.V. Bearing fault detection using Thomson's multitaper periodogram. *2018 Second International Conference on Intelligent Computing and Control Systems (ICICCS)*. 2018:1135–1139. <https://doi.org/10.1109/ICCONS.2018.8663183>
24. Gao Z., Jing Lin J., Wang X., Xu X. Bearing fault detection based on empirical wavelet transform and correlated kurtosis by acoustic emission. *Materials*. 2017;10(6):571. <https://doi.org/10.3390/ma10060571>
25. Polubaryev I.N., Dvoryaninov I.N., Saliev E.R. Experimental verification of a new approach to determining the loads acting on ball radia. *Forum Molodyh Uchenyh*. 2017;9(13):591–600.